Mausam, (1987), 38, 1, 43-48

551.465 : 551.553.21

The observed variability of the cooling and deepening of the mixed layer in the central Arabian Sea during Monsoon-77

R. R. RAO

Naval Physical & Oceanographic Laboratory, Cochin

(*Received 7 August 1984*)

सार — मिश्रित स्तर के ऊष्मा बजट का विश्लेषण करने से पता चला है कि मानसून-77 के दौरान पांच सप्ताहों के बाद तक के ग्रीष्म मानसून के प्रारंभ और प्रभाव सहित केन्द्रीय अरब सागर में 2.3° सें. का सतह शीलतन, शीतल जलों के संरोहण और अभिवहन के योगदान की तुलना नेट महासागर सतह में अधिकता के कारण हुआ। 55 मी. गहराई में उसके सदृश मिश्रित स्तर के एक प्रमुख भाग की, सतह शीतलन के एक आगामी प्रभाव द्वारा व्याख्या की गई जो संवहनी उलट की ओर अग्रसर करती है। सतही नेट ऊष्मा क्षति के एकमात्र प्रभाव के अन्तर्गत दोनों चरणों में 0.1° सें. की मूल माध्य वर्ग त्रुटि (आर.एम.एस.) सहित प्रेक्षित शीतलन और क्रमश : चरण I और II में 2.8 मी. और 6.3 मी. की अनुरूप त्रुटि सहित गहराई के सरल मौसम पूर्वानुमानी अभिकलनों का अनुकरण किया गया हैं।

ABSTRACT. Heat budget analysis of the mixed layer indicated that the surface cooling of 2.3° C in the central Arabian Sea with the onset and sway of the summer monsoon over five weeks during MONSOON-77 was mostly due to the net ocean surface losses as compared with the contributions of entrainment and advection of colder waters. A major portion of the corresponding mixed layer deepening of 55 m is explained by the one dimensional forcing of surface cooling leading to convective turnover. Under the only forcing of surface net heat loss, simple prognostic calculations simulated the observed cooling with a r.m.s error of 0.1 °C in both the phases and deepening with the corresponding error of 2.8 m and 6.3 m in phases I and II respectively.

1. Introduction

The seasonal onset and sway of summer monsoon cools and deepens the mixed layer of the Arabian Sea with varying magnitudes. The cooling is of the order of 10° C in the western, 4° to 5° C in the central and 2° C in the eastern Arabian Sea (INDEX 1977). Maximum deepening of the order of 60-80 m occurs in the central Arabian Sea (around 10° N & 60° E) and the layer depth reduces radially towards the coasts (Robinson *et al.* 1979). Several workers have attempted to explain the observed drop in the surface temperature. Colon (1964) proposed that increased cloudiness (reducing the solar radiation at the sea surface) and evaporation as the primary factors (contributing to the observed cooling in the eastern Arabian Sea. Saha (1974) hypothesized that following the coastal upwelling off Somalia and Arabia coasts, during late May or early June, a wedge of cold water is advected across the central Arabian Sea by the southwest monsoon current. Düing and Leetma (1980) computed the heat budget of the upper layers of the Arabian Sea and attributed upwelling as the dominant factor responsible for the observed summer monsoonal surface cooling in the western Arabian Sea. Krishnamurthi (1981) suggested that the surface cooling of the central and eastern (50° to 70° E) Arabian Sea around 10° N during June '79 was mostly governed by mid-oceanic upwelling caused by the positive curl of the surface wind stress associated with the summer monsoonal onset. Mc Phaden's (1982) mixed layer analysis indicated that about 80% of the observed variance in mixed layer temperature on monthly time scales in the central equatorial Indian Ocean can be accounted for by observed surface heat flux. Ramesh Babu and Sastry (1984) concluded that the downward transfer of heat due to the mixing of warm surface and cold sub-surface waters associated with increased current shear is the predominant process responsible for the observed cooling in the central and eastern Arabian Sea.

The mixed layer deepening is mostly attributed to mixing caused by wind and wave action, by convective turn over caused by the surface buoyancy flux inducing entrainment of colder waters from below, by increased current shear in the vertical across the base of the mixed layer and by quasi-geostrophic anticyclonic motion in the surface layer induced by the curl of the surface wind stress etc. These arguments imply that different processes assume differential importance at different geographic locations of the Arabian Sea. However, no definite quantitative figures are available to resolve the importance of various processes that are identified to explain the observed cooling and deepening of the mixed layer. The main lacune for this a situation is the lack of adequate time series measurements of temperatures made in the upper layers of the Arabian Sea during the summer monsoon season. Fortunately this has been partially overcome with the systematic collection of time series of surface marine meteorological parameters and BT data by deploying ships at selected areas of the Arabian Sea under different regimes

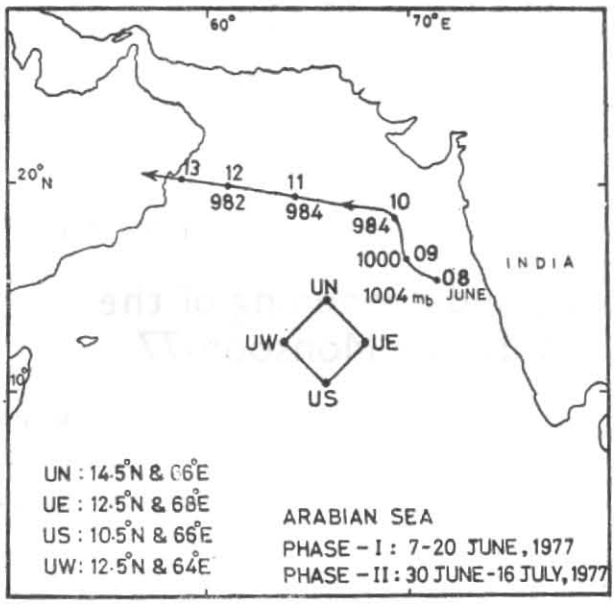

Fig. 1. Station location map with the track of the onset vortex system

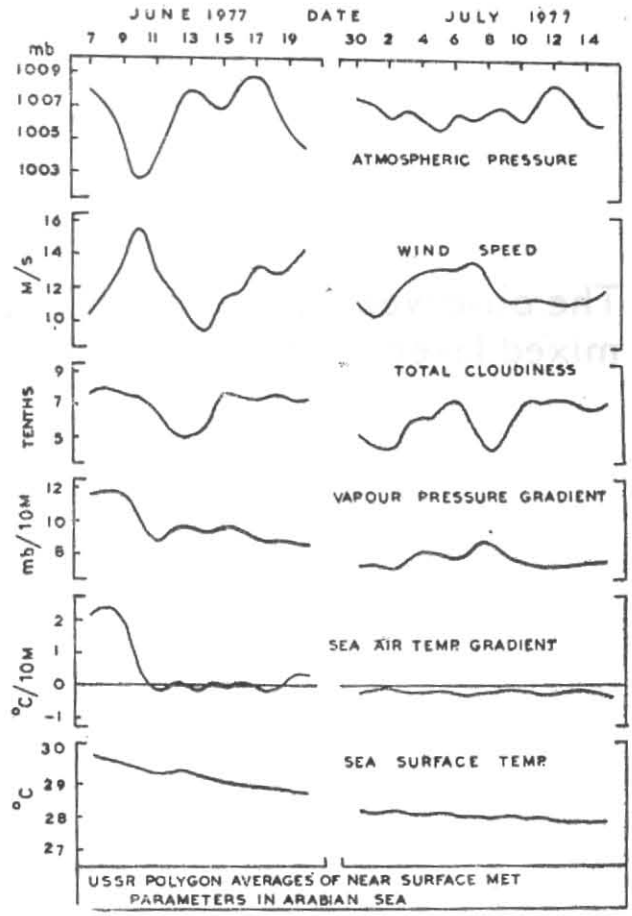

Fig. 2. Daily variation of he polygon averaged near surface marine meteorological parameters

of the summer monsoon during the recent summer Monsoon Experiments (ISMEX-73, MONSOON-77 and MONEX-79). In the present exercise advantage is taken of the time series data collected from a stationary USSR ship polygon over the central Arabian Sea during MONSOON-77 to parameterize some of the known processes responsible for the observed drop in SST and to link it with deepening of the layer.

2. Data

Four USSR ships were deployed as a stationary polygon over the central Arabian Sea. The geographic locations of the ships are shown in Fig. 1. Measurements of solar radiation and all standard surface marine meteorological parameters at hourly intervals, BT and salinity measurements at 3 hourly intervals were made during two phases of the observational schedule.

Phase I : 7-20 June 1977

Phase II : 30 June-15 July 1977

These data collected over a five week period provide an unique opportunity to examine the observed variability of the upper ocean thermal structure under the observed atmospheric forcing regimes. Daily averages of marine meteorological parameters and BT data at all the four ships are averaged to represent the polygon average. Some preliminary studies using some of these data were reported by Ramanadham *et al.* (1981), Rao (1982) and Rao *et al.* (1985).

3. Analysis and discussion

The polygon averaged marine meteorological parameters representative of surface meteorological forcing are shown in Fig. 2. In general larger fluctuations were observed during the disturbed meteorological conditions. Sharp variations in the surface pressure (drop of 5 mb), wind speed (increase of nearly 6 m/s), vapour pressure gradient (drop of 2.5 mb) and sea *minus* air temperature (drop over 2° C) are associated with the onset vortex system (track shown in Fig. 1) during 8 to 12 June. After the passsage of the system retreat to pre-onset conditions is evident only in the surface pressure. After the monsoonal onset sea *minus* air temperature continued to remain near zero value implying neutral equilibrium conditions to have prevailed. Sea surface temperature progressively cooled throughout with time. During Phase II the variations were relatively less violent as near steady state conditions were set in the monsoonal flow.

The progressive evolution of thermal profiles in the topmost 200 m layer averaged for the polygon area is shown in Fig. 3. During the five week period from 7 June 1977 the mixed layer cooled by 2.3° C and deepened by 55 m. However, the cooling and the deepening rates are higher in June compared to those in July implying that oceanic response is relatively stronger during the disturbed onset conditions of the monsoon compared to that of the steady state monsoonal sway. An inference may be drawn here that the cooling and the deepening of the mixed layer might have also been mostly influenced by the atmospheric forcing which is relatively stronger during the burst of the onset event. This would be illustrated further in the following discussion :

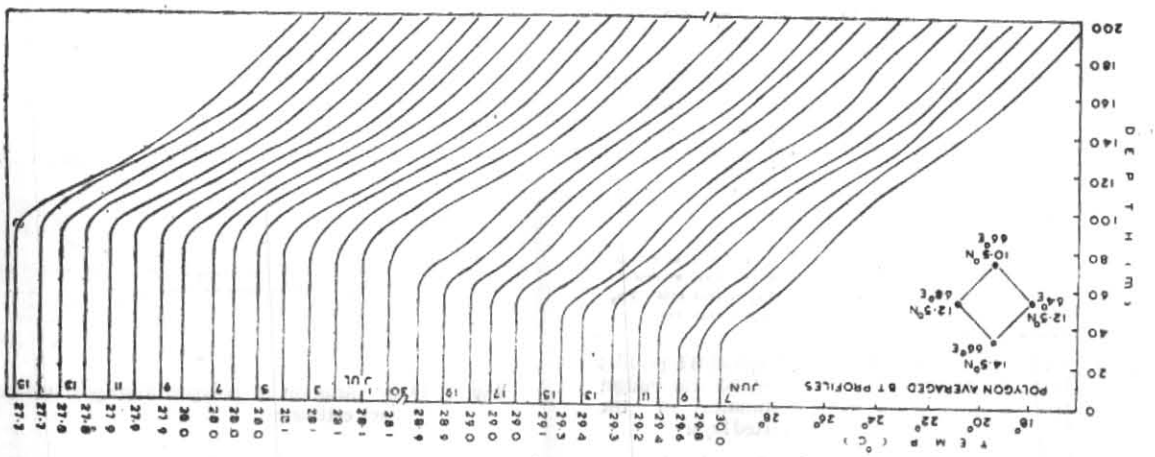

Fig. 3. Daily variation of polygon averaged BT profiles

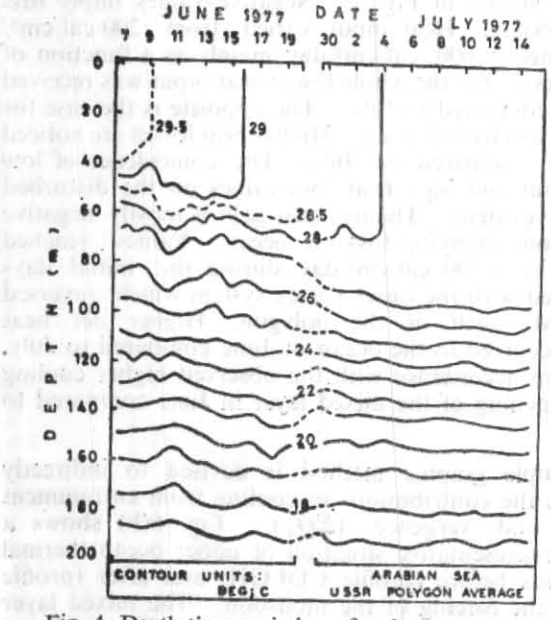

Fig. 4. Depth-time variation of polygon averaged temperature of the top 200 m layer

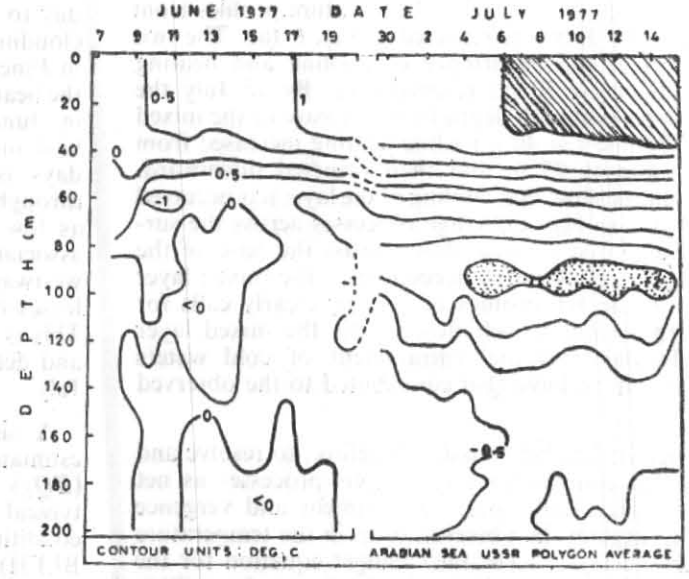

Fig. 5. Depth-time variation in the deviation of thermal field from that of initial day (7 June 1977)

The observed thermal structure in the top 200 m layer averaged for the polygon area is shown in Fig. 4. Isotherms are contoured at 1° C interval through linear interpolation in both depth and time domains. The progressive cooling and deepening of the near surface mixed layer is clearly seen. Below mixed layer in the upper thermocline, a progressive downwelling of isotherms with higher rate in June over July is also noticed. The average rate of down-welling reduced with depth. For instance 27° C isotherm descended by 30 m during the five week period implying an approximate sinking of 75 cm/day. The corresponding figure for 17° C isotherm is less than one third of the above. Yoshida and Mao (1957) have linked up the observed vertical velocities below the base of the mixed layer with the prevailing wind stress curl. Rao (1984), Ramesh Babu and Sastry (1984) have shown the occurrence of negative (clockwise) wind stress curl estimated from the wind measurements made from the four corners of the polygon as a responsible mechanism promoting Ekman type of convergence leading to sinking below mixed layer (Yoshida and Mao 1957). The short period embedded waves in the thermocline may be attributed to inertial oscillations caused due to the monsoonal wind forcing (Pollard 1970).

To depict the thermal changes resulted in the top 200 m layer with the onset and sway of the monsoon over a five week period with respect to 7 June all the successive daily averaged BT data are subtracted from that of 7 June and the deviations are contoured and shown in Fig. 5. Positive values correspond to cooling and negative values to warming with respect to the thermal profile observed on 7 June. Progressive cooling of over 2° C in the top mixed layer is evident. During Phase II the cooling monotonically decreased from surface to 60 m depth. A corresponding warming below the layer is also seen prominently from end of Phase I. Highest warming of over 2° C and with reduced magnitude on either side in the vertical has occurred around 95 m during Phase II. These observed thermal changes clearly demonstrate that heat is effectively redistributed in the vertical under the monsoonal forcing. The probable mechanisms responsible for

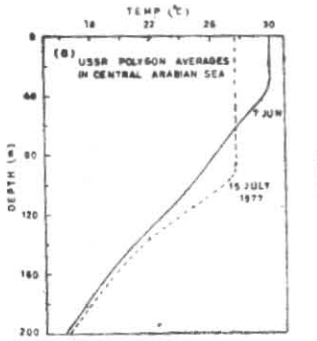

Fig. 6(a). BT profiles of initial and final days of observations

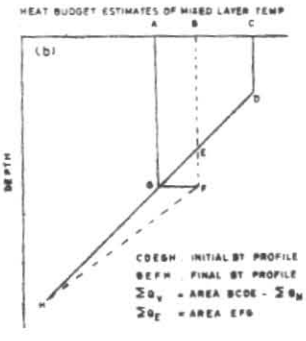

Fig. 6(b). Typical BT profiles for the heat budget estimates of the mixed layer

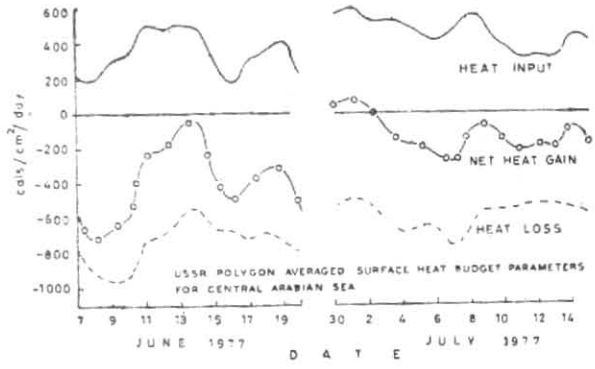

Fig. 7. Daily variation of polygon averaged surface heat budget estimates

these observed changes, *viz.*, cooling in the mixed layer and warming in the upper thermocline will be discussed later.

The changes in the vertical temperature profiles from 7 June to 15 July are reflected in Fig. 6 (a). The two profiles reveal the occurrence of cooling and heating above and below 60 m, respectively. By 15 July the cooling decreased with depth from the base of the mixed layer of 7 June ($\sim$ 40 m) while heating increased from 60 m to almost 95 m and then reversed downward. These changes show that cooling of the layer has occurred not only due to heat exchange processes across the surface but also due to heat flow across the base of the mixed layer. Penetrative deepening of the mixed layer reflected in the BT profiles of 15 July clearly calls for the incorporation of heat flow across the mixed layer base. In this case the entrainment of cold waters from below must have also contributed to the observed cooling.

An attempt has been made, therefore, to resolve and quantify the contributions of various processes as net oceanic surface heat loss, entrainment and vergence of heat to explain the observed drop in the temperature of the mixed layer. The heat budget equation for the mixed layer for each observed phase may be wtitten as

$$\frac{\partial T}{\partial t} = \left[\Sigma Q_N + \Sigma Q_E + \Sigma Q_V \right] \Big/ \rho c_p \bar{h} \quad (1)$$

where, $\partial T/\partial t$: change of temperature from beginning to the end of each phase.

ΣQ_N : cumulative net ocean heat gain/loss across the surface through all radiative and turbulent exchanges from beginning to the end of the phase.

ΣQ_E : cumulative entrainment of heat across the base of the mixed layer from beginning to the end of the phase.

ΣQ_V : cumulative lateral vergence of heat into the mixed layer from beginning to the end of the phase.

$\bar{h}$: phase averaged mixed layer depth.

The surface heat budget estimates from Rao *et al.* (1985) have been utilised for Q_N in this study. The distribution of heat input through insolation, of heat loss through net long wave radiation, of latent and sensible heat fluxes and of the net heat gain as a balance between these is shown in Fig. 7. Negative values imply loss to the ocean. Heat input varied from 200 cal/cm²/day to nearly 600 cal/cm²/day mainly as a function of cloudiness. On the whole lower heat input was received in June compared to July. The opposite is the case for the heat loss from the sea. Higher heat losses are noticed in June compared to July. The coincidence of low heat input and high heat loss values on the disturbed days is evident. The net heat gain is mostly negative throughout implying loss to ocean. Values reached as low as —700 cal/cm²/day during the initial days associated with the onset vortex system which traversed westward north of the polygon. Higher net heat losses occurred to the ocean in June compared to July. This is in accordance with the observed higher cooling and deepening of the mixed layer in June compared to July.

A simple graphic method is devised to indirectly estimate the contributions of cooling from entrainment (ΣQ_E) and vergence (ΣQ_V). Fig. 6(b) shows a typical representative situation of upper ocean thermal conditions before (profile CDEGH) and after (profile BEFH) the forcing of the monsoon. The mixed layer cooling might be equated to the graphically integrated difference in the heat contents of ABCDEGA and ABEFGA, *i.e.*, heat contents with respect to the temperature at G as the final BT profile showed the mixed layer deepening upto that depth. Excluding the common area ABEGA, areas BCDEB and EFGE are of interest. Here it is proposed that the heat content of BCDEB is to be equated to the sum of ΣQ_N and ΣQ_V. ΣQ_V is estimated as a residual term as ΣQ_N is derived with marine meteorological data. The heat content of EFGE is to be equated to the contribution of ΣQ_E. The cooling values from these individual estimates of ΣQ_N, ΣQ_E and $\Sigma' Q_V$ are shown in Table 1.

The sum of the computed cooling for each phase due to all these three processes is shown in the fourth row for comparison with the observed cooling of the mixed layer shown in the fifth row. The error as the difference between computed and observed cooling is shown in the last row. During Phase I surface heat fluxes and entrainment across the base of the mixed layer contributed to the cooling (the former being much higher) while the vergence of heat contributed to warming of the layer. This situation changed in Phase II only in

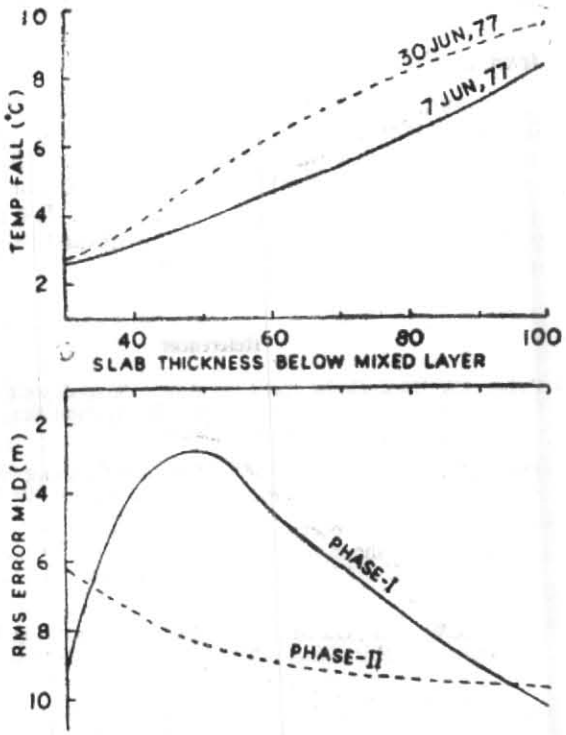

Fig. 8. Temperature drop below mixed layer in different slabs on 7 and 30 June 1977 and corresponding r.m.s. error in predicted MLD

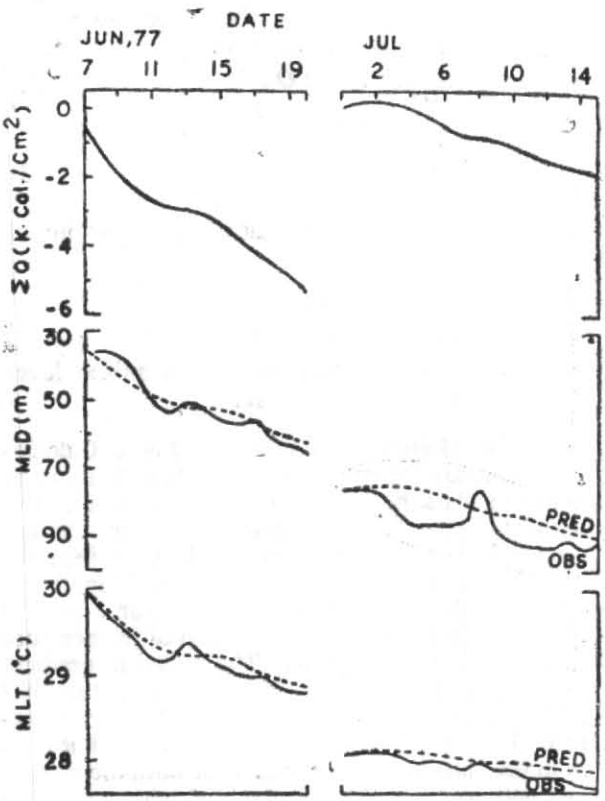

Fig. 9. Cumulative surface heat flux from 7 and 30 June and observed and predicted MLD and MLT

TABLE 1

Mixed layer cooling (°C) in the central Arabian Sea from heat budget estimates during MONSOON-77

	7– 20 June '77 (Phase I)					30 June – 15 July '77 (Phase II)				
	UN	UE	US	UW	$\bar{X}$	UN	UE	US	UW	$\bar{X}$
(1) ΣQ_N (Surface heat budget)	—1.18	—1.26	—0.83	—1.12	—1.10	—0.42	— 0.13	— 0.03	— 0.33	— 0.23
(2) ΣQ_E (Entrainment)	—0.47	—0.15	—0.20	—0.05	— 0.22	—0.23	—0.01	0.01	—0.03	—0.07
(3) ΣQ_V (Vergence)	0.23	0.40	—0.17	0.63	0.36	0.26	—0.26	—0.41	—0.14	—0.14
(4) $\Sigma Q_N + \Sigma Q_E + \Sigma Q_V$	—1.42	—1.01	—0.86	—0.54	—0.96	—0.39	—0.40	—0.44	—0.50	—0.43
(5) Obs. cooling	—1.24	—1.05	—0.77	—0.54	—0.90	—0.20	—0.42	—0.44	—0.50	—0.39
(6) Error	0.18	—0.04	0.10	0.00	0.06	0.20	—0.02	0.00	0.00	0.05

respect of vergence of heat with the only exception at the northern location of the polygon. During Phase I the cooling caused by surface heat exchange processes is five times of entrainment. This factor is reduced from five to three during Phase II. Rao (1982) inadvertantly ignored the influence of inertial oscillations while attributing entrainment as the dominant process responsible for the observed cooling. During Phase I heat gain due to convergence in the mixed layer may be accounted due to the prevailing thermal gradient from northwest to southeast (the average SST values for Phase I at northern and eastern corners of the polygon were 29.4° C and 29.0° C respectively), and southeasterly currents upto 100 m depth (Ramam *et al.* 1982). With no major change in the current pattern, the thermal gradient got reversed during Phase II (the average SST values for Phase II at northern and eastern corners of the polygon were 27.9° C and 28.2° C respectively). During Phase II the contribution of advection of colder waters has become relatively prominent (accounts one third of the observed cooling). This may indicate that advection of colder upwelled waters off Somalia and Arabia coasts becomes significant only after the atmospheric and oceanic flow patterns attain steady state conditions. The polygon averaged error estimates being mostly less than 0.1° C give considerable reliance on the scheme devised for the heat budget estimation of the mixed layer.

An attempt is made to simulate the observed cooling and deepening characteristics of the mixed layer with the following diagnostic calculations :

$$\mathrm{MLD}_{t+1} = \mathrm{MLD}_t + \frac{2\,Q_N}{\rho c_p \,\triangle T_I} \qquad (2)$$

$$\mathrm{MLT}_{t+1} = \mathrm{MLT}_t + \frac{Q_N}{\rho\, c_p\, \mathrm{MLD}_{t+1}} \qquad (3)$$

where the subscripts t and I indicate time and initial values respectively.

MLD : mixed layer depth

MLT : mixed layer temperature

$\triangle T_I$: drop of temperature just below mixed layer in a slab of thickness $\triangle z$.

Eqn. (2) from James (1966) is modified here. Calculations are repeated for different $\triangle z$ values from 10 m to 100 m to get the best estimates of layer depth. The calculations are made by considering the values $\triangle T_I$ on 7 June and 30 June as initial conditions for both the phases separately. Fig. 8 shows the temperature drop in the slab *versus* thickness ($\triangle z$) for 7 and 30 June. Almost linear increase in the drop of temperature with slab thickness is evident. The thermal gradient below mixed layer is sharper on 30 June over that of 7 June. The r.m.s. error in the predicted MLD with temperature drop ($\triangle T_I$) for different slab thickness is shown in the bottom panel of Fig. 8 for both the phases. Best predictions of MLD are obtained with $\triangle z = 50$ m for Phase I and $\triangle z = 30$ m for Phase II with corresponding temperature drops ($\triangle T_I$) of 3.9° C and 2.6° C respectively. Mixed layer depth is predicted using these observed temperature drops in the slabs of 50 m and 30 m respectively for 7 and 30 June as the initial bottom boundary conditions and the variable daily heat budget estimate Q_N. Predicted MLD is incorporated in Eqn. (3) to predict the MLT. Cumulative net surface heat gain from 7 and 30 June is shown in Fig. 9 for both the phases. In the bottom panel, observed and predicted MLD and MLT show a remarkable agreement in their slopes, thus pointing out the importance of surface heat exchanged in regulating MLD and MLT. The agreement between predicted and observed MLD during Phase I is significant. However, during Phase II the predicted layer depth is an under estimate of the observed. As the cooling is concerned, the agreement is also good though the predicted MLT is an over estimate of the observed. It is logical to conclude here that the surface heat losses cannot account for the total cooling as the other processes like entrainment and vergence also contribute to cooling.

4. Conclusions

(*i*) Polygon averaged mixed layer in the central Arabian Sea cooled by 2.3° C and deepened by 55 m with the onset and sway of the summer monsoon.

(*ii*) Cooling caused by net surface heat losses is found to be 3 to 5 times that of entrainment.

(*iii*) Advection of colder waters seems to assume importance only after the complete onset of the monsoon (*i.e.*, under steady state conditions)

(*iv*) Simple prognostic calculations incorporating only surface heat exchanges simulated the observed cooling and deepening remarkably well with small r.m.s. errors.

Acknowledgements

The author wishes to record his gratitude to Dr. D. Srinivasan for his encouragement and for providing facilities to carry out this investigation. Thanks are due to the Project Director, MONEX for making available all the data used in this study. The author is grateful to the referee who have contributed in sharpening the paper.

References

Colon, J.A., 1964, On interactions between the southwest monsoon current and the sea surface over the Arabian Sea, *Indian J. Met. Geophys.*, **15**, 2, pp. 183-200.

Duing, W. and Leetma, A., 1980, Arabian Sea cooling : A preliminary heat budget, *J. Phys. Oceanogr.*, **10**, pp. 302-312.

INDEX, 1977, An oceanographic contribution to international progress in the monsoon region of the Indian Ocean, Report No. 1D 075-01571, National Science Foundation, Washington, D.C.

James, R.W., 1966, Ocean thermal structure forecasting, US Naval Oceanographic Office, ASWEPS Manual Services SP 105, Vol. 5, Washington, D.C.

Kondo, J., 1975, Air Sea bulk transfer coefficents in diabatic conditions, *Bondary Layer Met.*, **9**, pp. 91-112.

Krishnamurthi, T.N., 1981, Cooling of the Arabian Sea and onset vortex during 1979, Recent Progress in Equatorial Oceanography, A report of the final meeting of SCOR working Group 47 in Venice, Italy.

Mc Phaden, M.J., 1982, Variability in the central equatorial Indian Ocean, Part II : Oceanic heat and turbulent energy balance, *J. Marine Res.*, **40**, 2, pp. 403-419.

Polland, R.T., 1972, On the generation by winds of inertial waves in the ocean, *Deep Sea Res.*, **17**, pp. 795-812.

Ramam, K.V.S., Prasada Rao, C.V.K. and Durga Prasad, N., 1982, On the time varying currents and hydrographic conditions in the central Arabian Sea during summer MONSOON-77, *Mausam*, **33**, 4, pp. 451-458.

Ramesh Babu, V. and Sastry, J.S., 1984, Summer cooling in the east central Arabian Sea—A process of dynamic response to the southwest monsoon, *Mausam*, **35**, 1, pp. 17-26.

Rao, R.R., 1982, On the space-time variability of heat budget estimates of ocean surface mixed layer and thermal structure of upper 200 m in the central Arabian Sea during MONSOON-77, Proceedings of International Conference on the Scientific Results of the Monsoon Experiment held at Bali, Indonesia, Oct 1981, pp. (7), 39-42.

Rao, R.R., 1984, On the thermal response of the upper central Arabian Sea to the summer monsoonal forcing during MONSOON-77, Communicated to *Mausam*.

Rao, R.R., Ramam, K.V.S., Rao, D.S. and Joseph, M.X., 1985, Surface heat budget estimates at selected areas of north Indian Ocean during MONSOON-77, *Mausam*, **36**, 1, pp. 21-32.

Robinson, M.K., Bauer, R.A. and Sohroeder, E.H., 1979, Atlas of North Atlantic-Indian Ocean monthly mean temperatures and mean salinities of the surface layers, Naval Oceanographic Office Reference publication 18, Dept. of the Navy, Washington, D.C. 20373.

Saha, K.R., 1974, Some aspects of the Arabian Sea summer monsoon, *Tellus*, **XXVI**, 4, pp. 464-476.

Yoshida, K. and Maok, H.L., 1957, A theory of upwelling of large horizontal extent, *J. Mar. Res.*, **16**, pp. 40-57.